

DESY-00-011  
 RAL-TR-1999-073  
 Nov 1999

# The triple Higgs self-coupling at future $e^+e^-$ colliders: a signal-to-background study for the standard model<sup>1</sup>

D.J. MILLER<sup>1</sup> and S. MORETTI<sup>2</sup>

*1) Deutches Elektronen-Synchrotron DESY, D-22603 Hamburg, Germany*

*2) Rutherford Appleton Laboratory, Chilton, Didcot, Oxon OX11 0QX, UK.*

## Abstract

The experimental reconstruction of the Higgs self-energy potential is essential to a verification of the Higgs boson's rôle in spontaneous electroweak symmetry breaking. The first step towards this goal, the measurement of the triple Higgs self-coupling, can possibly be accomplished at the next generation of linear colliders. Here we present a background study of the most promising channel, double Higgs-strahlung off a  $Z$  boson,  $e^+e^- \rightarrow HHZ$ , with the subsequent decay  $H \rightarrow b\bar{b}$ , and evaluate the feasibility of its measurement.

## 1 Introduction

To verify whether or not the Higgs mechanism is responsible for spontaneous electroweak symmetry breaking as expected by the standard model (SM), or indeed, the minimal supersymmetric standard model (MSSM), one must perform an experimental reconstruction of the Higgs self-energy potential. This reconstruction requires the measurement of the Higgs boson mass(es) and the triple and quartic Higgs self-couplings. The triple Higgs self-coupling may become accessible to direct measurement at an electron-positron linear collider (LC) with centre-of-mass energy at the TeV scale. In this study we compare the signal of the most promising channel with its dominant electroweak (EW) and QCD backgrounds to assess the feasibility of its measurement.

---

<sup>1</sup>Talk given at the Fourth Workshop of the “*2nd Joint ECFA/DESY Study on Physics and Detectors for a Linear Electron-Positron Collider*,” Oxford, UK, 20-23 March 1999.

We restrict ourselves to a discussion of the triple Higgs self-coupling in the SM<sup>2</sup> and in particular double Higgs-strahlung off  $Z$  bosons, in the process  $e^+e^- \rightarrow HHZ$ . We adopt the  $H \rightarrow b\bar{b}$  decay channel over the Higgs mass range  $M_H \lesssim 140$  GeV and assume very efficient tagging and high-purity sampling of  $b$  quarks. Then the backgrounds to the  $\lambda_{HHH}$  measurement are primarily the ‘irreducible’ EW and QCD backgrounds  $e^+e^- \rightarrow b\bar{b}b\bar{b}Z$ .

The EW background is of  $\mathcal{O}(\alpha_{em}^5)$  away from resonances, but can, in principle, be problematic due to the presence of both  $Z$  vectors and Higgs scalars yielding  $b\bar{b}$  pairs. In contrast, the QCD background is of  $\mathcal{O}(\alpha_{em}^3\alpha_s^2)$ . Here, although there are no heavy objects decaying to  $b\bar{b}$  pairs, the production rate itself could give difficulties due to the presence of the strong coupling. In addition, the double Higgs-strahlung process (see Fig. 2) contains diagrams proceeding via an  $HHZ$  intermediate state but not dependent on  $\lambda_{HHH}$ , as well as a diagram sensitive to the triple Higgs self-coupling (the right-hand graph of Fig. 2).

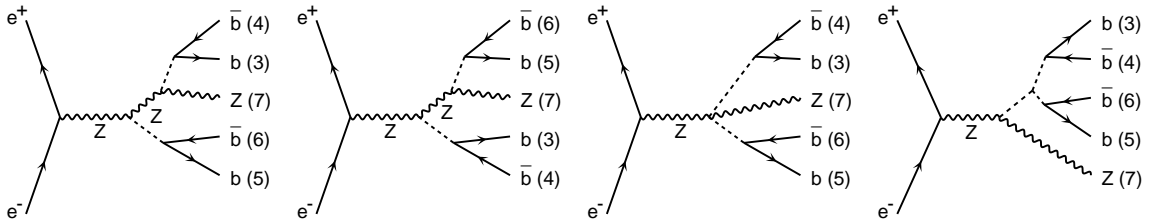


Figure 1: Diagrams contributing at lowest-order to  $e^+e^- \rightarrow b_{(3)}\bar{b}_{(4)}b_{(5)}\bar{b}_{(6)}Z_{(7)}$  via purely EW interactions containing two Higgs bosons in the intermediate state. Note that only the far right diagram contains a dependence on  $\lambda_{HHH}$ .

The plan of the paper is as follows. The next section details the procedure adopted in computing the relevant scattering amplitudes. Section 3 displays our numerical results and contains our discussion. Finally, in the last section, we summarize and conclude.

## 2 The calculation

The signal process is rather straightforward to calculate in the case of on-shell  $HHZ$  production (see Ref. [2] for an analytic expression of the matrix elements (MEs)). The EW

<sup>2</sup>Some of the trilinear couplings of the MSSM may prove to be accessible even at the LHC via resonant decay of a heavy Higgs, eg.  $H \rightarrow hh$ , and are under investigation elsewhere [3].

background is more complex, deriving from many graphs with different resonant structures. In order to perform an efficient integration we have grouped the Feynman diagrams into different collections of diagrams with identical (non-)resonant structure. This categorization allows one to compute each of the topologies separately, with the appropriate mapping of variables, thus optimizing the accuracy of the numerical integration. Furthermore, one is able to assess the relative weight of the various subprocesses in the full scattering amplitude, giving added insight into the fundamental dynamics. In contrast the QCD background contains fewer diagrams, with only five different (non-)resonant topologies. This makes integration much simpler than in the EW case and it can be carried out with percent accuracy directly over the full ME using standard multichannel Monte Carlo methods. For further details and numerical inputs see Ref. [4].

We assume that total and differential rates are those at the partonic level, as we identify jets with the partons from which they originate. To resolve the final state  $b$  (anti)quarks as separate systems, we impose the following acceptance cuts:  $E(b) > 10$  GeV on the energy of each  $b$  (anti)quark and  $\cos(b, b) < 0.95$  on the relative separation of all possible  $2b$  combinations. We further assume that  $b$  jets are distinguishable from light-quark and gluon jets (by using, for example,  $\mu$ -vertex tagging techniques). However, no efficiency to tag the four  $b$  quarks is included in our results. The  $Z$  boson is treated as on-shell and no branching ratio is applied to quantify its possible decays. In practice, in order to simplify the treatment of the final state, one may assume that the  $Z$  boson decays leptonically (that is,  $Z \rightarrow \ell^+ \ell^-$ , with  $\ell = e, \mu, \tau$ ) or hadronically into light quark jets (that is,  $Z \rightarrow q\bar{q}$ , with  $q \neq b$ ). Also, we have not included Initial State Radiation (ISR) [5] in our calculations.

### 3 Results

The total signal cross section is plotted as a function of  $M_H$  in the top-left frame of Fig. 2, for three centre-of-mass (CM) energies. Even at low Higgs masses where both the production and decay rates are largest, the signal is rather small. In fact, the signal is below 0.2 femtobarns for all energies from 500 to 1500 GeV, although this can be doubled simply by polarizing the incoming electron and positron beams. Thus, as already recognized in Ref. [2], where on-shell production studies of the signal were performed, luminosities of the order of one inverse attobarn need to be collected before statistically significant measurements of  $\lambda_{HHH}$  can be performed.

The decrease of the signal with increasing Higgs mass is due to suppression of the  $H \rightarrow b\bar{b}$  decay channel. Above  $M_H \approx 140$  GeV it becomes overwhelmed by the opening of the off-shell  $H \rightarrow W^{\pm*}W^{\mp}$  decay (see, for example, Fig. 1 of Ref. [6]). In contrast, the production cross section for  $e^+e^- \rightarrow HHZ$  without specifying the subsequent decay is much less sensitive to  $M_H$  [2]. In addition, because the signal is an annihilation process proportional to  $1/s$ , a larger CM energy ( $E_{\text{cm}}$ ) tends to deplete the production rates, as long as  $E_{\text{cm}} \gg 2M_H + M_Z$ . When this is no longer true, e.g., at 500 GeV and  $M_H \gtrsim 140$  GeV, phase space suppression can overturn the  $1/s$  propagator effects. This is evidenced by the crossing of the curves for 500 and 1000 GeV in Fig. 2.

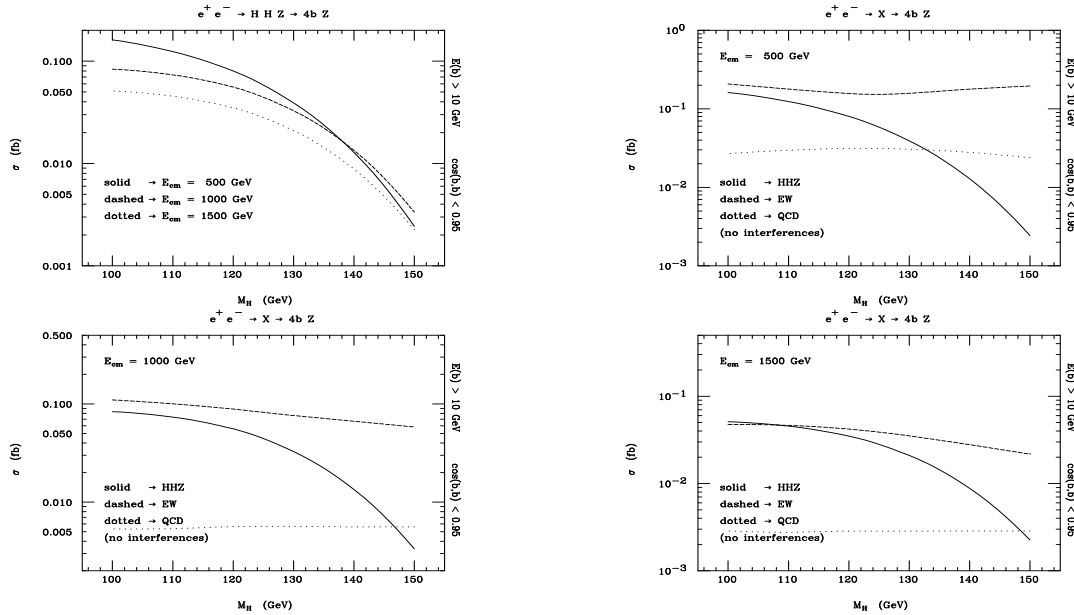


Figure 2: Top-left: cross sections in femtobarns for the signal at three different collider energies: 500, 1000 and 1500 GeV. Top-right(Bottom-left)[Bottom-right]: cross sections in femtobarns for the signal versus the EW and QCD backgrounds at 500(1000)[1500] GeV. Our acceptance cuts in energy and separation of the four  $b$  quarks have been implemented.

Fig. 2 also shows the background processes plotted with respect to  $M_H$  for the three CM energies. As anticipated, the EW background is problematic due to its resonance structures, whereas the QCD background presents no such difficulty and does not significantly obscure the signal, despite the strong coupling constant. Our categorization of the EW background into different resonant topologies now facilitates a closer examination. In particular we observe that only four sub-processes dominate the background. Generic

Feynman diagrams of these sub-processes can be seen in Fig. 3, together with their contribution to the total EW background rate, as a function of the Higgs boson mass. All other EW sub-processes are much smaller, rarely exceeding  $10^{-3}$  femtobarns, and have little effect on the kinematics or magnitude of the background.

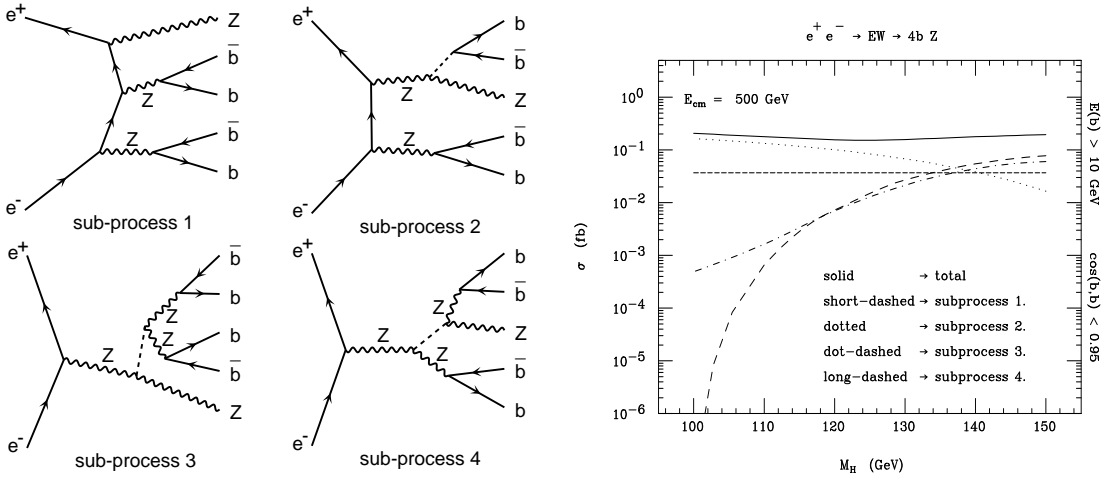


Figure 3: On the left, generic Feynman diagrams representing the four dominant EW topologies. Note that only sub-process 1 does not contain a Higgs boson in the intermediate state. The different contributions of these sub-processes to the total EW background are displayed in the plot to the right, as a function of the Higgs boson mass.

The QCD background is dominated by  $e^+e^- \rightarrow ZZ$  production with one of the two  $Z$  bosons decaying hadronically into four  $b$  jets. Also significant is single Higgs-strahlung production (off a  $Z$ ) with the Higgs scalar subsequently decaying into  $b\bar{b}b\bar{b}$  via an off-shell gluon. The contributions of the other diagrams, which do not resonate, are typically one order of magnitude smaller than the  $ZZ$  and  $ZH$  mediated graphs, with the interferences smaller still (and generally negative).

We now investigate several differential spectra, to find kinematic cuts which will suppress the backgrounds. The distributions in  $E(b)$  and  $\cos(b, b)$  cannot be further exploited after the acceptance cuts are made. Instead we consider the invariant masses of  $b$  (anti)quark systems: for  $2b$  systems where the  $b$  jets come from the same production vertex ('right' pairing) or otherwise ('wrong' pairing); for  $3b$  systems, and for the  $4b$  system. The spectra for the  $2b$  and  $4b$  systems are shown in Fig. 4 (the  $3b$  spectra are less useful and are

not shown here). It is clear that the narrow Higgs peak<sup>3</sup> in the  $M_R(bb)$  distribution, can be exploited to reduce the QCD background. Although the EW process also displays a resonance at  $M_H$ , only one  $2b$  invariant mass will peak here compared to two combinations in the signal. The EW background can therefore also be cut away. Finally, one may require that none of the  $2b$  invariant masses reproduce a  $Z$  boson, provided that the invariant mass resolution of di-jet systems is at least as good as the difference  $(M_H - M_Z)/2$ , in order to resolve the  $Z$  and  $H$  peaks. The  $M(bbbb)$  spectra is also useful in distinguishing signal from background since clearly  $M(bbbb)$  must always be greater than  $2M_H$  for the signal process, while it can be lower for both background processes (especially for the QCD background).

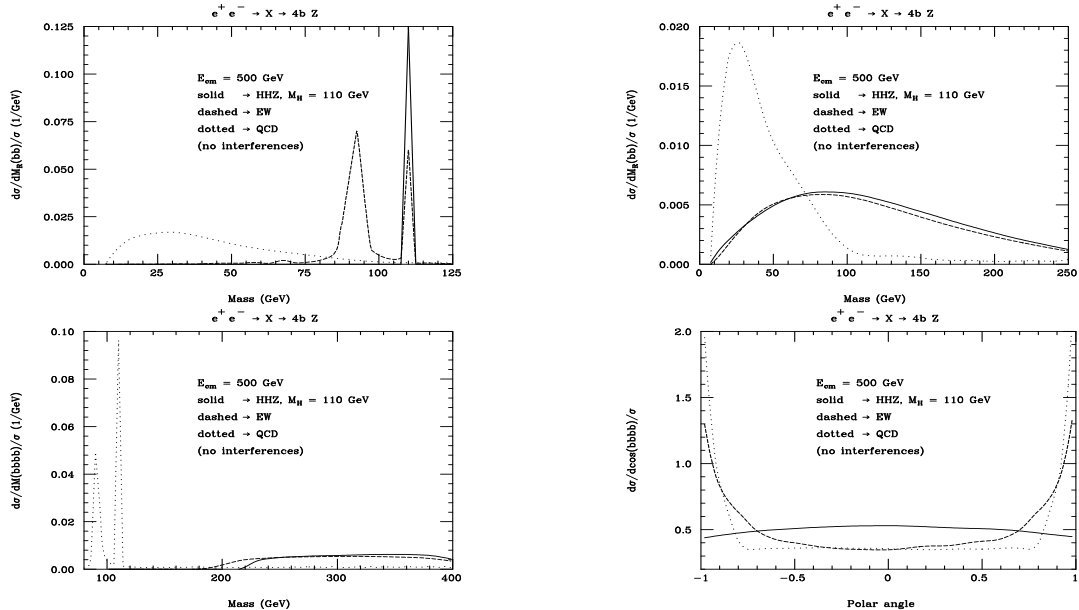


Figure 4: Differential distributions in invariant mass of multi-jet systems containing two or four  $b$  (anti)quarks. Also shown in the bottom right plot is the (cosine of) the angle of the  $4b$  system with respect to the beam axis. The CM energy is 500 GeV and the Higgs mass 110 GeV. Our acceptance cuts in energy and separation of the four  $b$  quarks have been implemented.

In addition to the different resonance structures of signal and background one can exploit the dominantly  $t$ -channel nature of the backgrounds as compared to the  $s$ -channel

<sup>3</sup>Recall that for  $M_H = 110$  GeV one has  $\Gamma_H \approx 3$  MeV. The Higgs resonances in Fig. 4 are smeared by incorporating a 5 GeV bin width.

signal. In Fig. 4 we also show the cosine of the polar angle (i.e. with respect to the beam axes) of the four  $b$  quark system (or, indeed, the real  $Z$ ). Notice that the backgrounds are much more forward peaked than the signal. The QCD events are predominantly  $e^+e^- \rightarrow ZZ$  production followed by the decay of one of the gauge bosons into four  $b$  quarks. The  $ZZ$  pair is produced via  $t, u$ -channel graphs so the four  $b$  quarks are preferentially directed forwards and backwards into the detector. In contrast, the signal is entirely  $s$ -channel resulting in more centrally produced  $b$  jets. The EW background has a more complicated structure but is still sizably dominated by forward production. A similar effect is seen for  $\cos(bbb)$  and  $\cos(bb)$ , allowing one to separate signal and backgrounds events efficiently.

The transverse momentum distributions of the  $4b$ ,  $3b$  and  $2b$  systems were also examined. However the distributions for the signal and the EW background proved too similar to allow their use as efficient kinematic variables for cuts.

The main features of distributions studied above are rather stable to variation of the CM energy or Higgs mass (within the ranges under discussion). We can therefore optimize the  $S/B$  ratio by imposing the cuts:

$$|M(bb) - M_H| < 5 \text{ GeV} \text{ (on exactly two combinations of } 2b \text{ systems),}$$

$$|M(bb) - M_Z| > 5 \text{ GeV} \text{ (for all combinations of } 2b \text{ systems)}$$

$$M(bbbb) > 2M_H, \quad |\cos(2b, 3b, 4b)| < 0.75. \quad (1)$$

In enforcing these constraints, we assume no  $b$  jet charge determination.

The signal and background cross-sections after the implementation of the selection cuts can be seen in Fig. 5. Both background rates are greatly reduced while a large portion of the original signal is maintained. This results in a  $S/B$  ratio which is enormously large for not too heavy Higgs masses. For example, at Centre-of-mass energies  $E_{\text{cm}} = 500(1000)[1500]$  GeV and for  $M_H = 110$  GeV, one finds  $S/B = 25(60)[104]$ . This remarkable suppression of the backgrounds comes largely from the invariant mass cuts on  $M_{bb}$ . In fact, they are crucial not only in selecting the  $M_H$  resonance of the signal, but also in minimizing the signal rejection around  $M_Z$  when mispairings occur: notice the shoulder at 90 GeV of the  $M_W(bb)$  signal spectrum.

A number of caveats to our analysis apply. Firstly, the value we have adopted for the resolution is rather high, considering the large uncertainties normally associated with the experimental determination of jet angles and energies, though not unrealistic in view

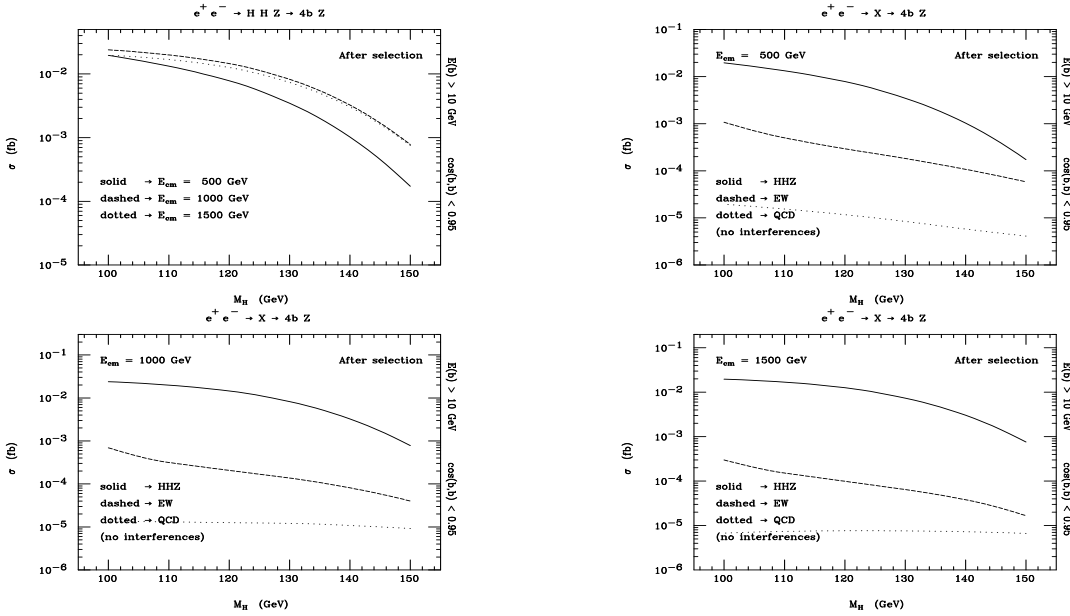


Figure 5: Top-left: cross sections in femtobarns for the signal at three different collider energies: 500, 1000 and 1500 GeV. Top-right(Bottom-left)[Bottom-right]: cross sections in femtobarns for the signal versus the EW and QCD backgrounds at 500(1000)[1500] GeV. Acceptance and selection cuts have been implemented.

of the most recent studies [7]. The ability of the actual detectors in guaranteeing the performances foreseen at present is thus crucial for the feasibility of dedicated studies of double Higgs-strahlung events at the LC. Furthermore, one must consider the efficiency of tagging the  $b$  quarks necessarily present in the final state, particularly in the case in which the  $Z$  boson decays hadronically. Given the high production rate of six jet events from QCD [8] and multiple gauge boson resonances [9] in light quark and gluon jets, it is desirable to resort to heavy flavour identification in hadronic samples. However, the poor statistics of the  $HHZ$  signal requires a judicious approach in order not to deplete it below detection level. According to recent studies [10], the two instances can be combined successfully, as efficiencies for tagging  $b\bar{b}$  pairs produced in Higgs decays were computed to be as large as  $\epsilon_{b\bar{b}} \approx 90\%$ , with mis-identification probabilities of light(charmed) quarks as low as  $\epsilon_{q\bar{q}(c\bar{c})} \approx 0.3(4)\%$  (and negligible for gluons). If such a projection for the LC detectors proves to be true, then even the requirement of tagging exactly four  $b$  quarks in double Higgs-strahlung events might be statistically feasible, thus suppressing the reducible backgrounds to really marginal levels [11]. One should also bear in mind that experimental considerations, such

as the performances of detectors, the fragmentation/hadronization dynamics and a realistic treatment of the  $Z$  boson decays, are also important when determining what cuts should be made. Such considerations are beyond the scope of this paper, and are under study elsewhere [11].

Finally, the number of signal and backgrounds events seen per inverse attobarn of luminosity at  $E_{\text{cm}} = 500, 1000$ , and  $1500$  GeV, with  $M_H = 110$  GeV, can be seen in Tab. 1. One could relax one or more of the constraints we have adopted to try to improve the signal rates without letting the backgrounds become unmanageably large. However, such a relaxation only marginally effects the signal while significantly reducing the  $S/B$  ratio, and should only be done if high luminosities cannot be obtained. Kinematic fits can also help in improving the  $S/B$  ratio [11].

	Number of Events per $ab^{-1}$ after selection cuts		
	$E_{\text{cm}} = 500$ GeV	$E_{\text{cm}} = 1000$ GeV	$E_{\text{cm}} = 1500$ GeV
signal	26	40	34
Electroweak	1.0	0.6	0.3
QCD	0.032	0.026	0.016

Table 1: The number of events for signal and backgrounds per inverse attobarn of luminosity after selection cuts for centre-of-mass energies of 500, 1000 and 1500 GeV, a Higgs mass of 110 GeV, and with polarized electron and positron beams.

## 4 Summary

In conclusion, the overwhelming irreducible background from Ew and QCD processes of the type  $e^+e^- \rightarrow b\bar{b}b\bar{b}Z$  to double Higgs production in association with  $Z$  bosons and decay in the channel  $H \rightarrow b\bar{b}$ , i.e.,  $e^+e^- \rightarrow HHZ \rightarrow b\bar{b}b\bar{b}Z$ , should easily be suppressed down to manageable levels by simple kinematics cuts: e.g. in invariant masses and polar angles.

The number of signal events is generally rather low, but will be observable at the LC provided that it provides very high luminosity, excellent  $b$  tagging performances, and high di-jet resolution. As advocated in Ref. [11], one also requires a good forward acceptance for jets since single jet directions in the double Higgs-strahlung process can stretch up to about  $20^\circ$  in polar angle.

## References

- [1] Proceedings of the Workshop  *$e^+e^-$  Collisions at 500 GeV. The Physics Potential*, Munich, Annecy, Hamburg, 3–4 February 1991, ed. P.M. Zerwas, DESY 92–123A/B, August 1992, DESY 93–123C, December 1993;  
E. Accomando et al., *Phys. Rep.* **299**, (1998) 1.
- [2] A. Djouadi, W. Kilian, M. Mühlleitner and P.M. Zerwas, *Eur. Phys. J.* **C10** (1999) 27; contribution to the XXIX *International Conference on High Energy Physics*, Vancouver 1998, Heidelberg Report HD-THEP 98-29.
- [3] R. Lafaye, D. J. Miller, S. Moretti and M. Mühlleitner, contribution to proceedings of workshop on “Physics at TeV Colliders”, Les Houches, France 8-18 June 1999.
- [4] D. J. Miller and S. Moretti, June 1999, [hep-ph/9906395](https://arxiv.org/abs/hep-ph/9906395).
- [5] T. Barklow, P. Chen and W. Kozanecki, in Ref. [1], part A.
- [6] Z. Kunszt, S. Moretti and W.J. Stirling, *Z. Phys.* **C74** (1997) 479.
- [7] F. Richard, private communication.
- [8] S. Moretti, *Phys. Lett.* **B420** (1998) 367; *Nucl. Phys.* **B544** (1999) 289.
- [9] A. Aeppli *et. al.*, in Ref. [1], part A;  
V. Barger and T. Han, *Phys. Lett.* **B212** (1988) 117;  
V. Barger, T. Han and R.J.N. Phillips, *Phys. Rev.* **D39** (1889) 146;  
A. Tofighi-Niaki and J.F. Gunion, *Phys. Rev.* **D39** (1989) 720.
- [10] G. Borissov, talk delivered at the ECFA/DESY Workshop on “Physics and Detectors for a Linear Collider”, Oxford, UK, March 20–23, 1999;  
M. Battaglia, *ibidem*.
- [11] P. Lutz, talk delivered at the ECFA/DESY Workshop on “Physics and Detectors for a Linear Collider”, Oxford, UK, March 20–23, 1999.